Production of $2\,^3S_1$ positronium atoms by single-photon excitation in an electric field

A. M. Alonso, S. D. Hogan, and D. B. Cassidy

Department of Physics and Astronomy, University College London, Gower Street, London WC1E 6BT, United Kingdom

We report experiments in which positronium (Ps) atoms are produced in the $2\,^3S_1$ level by single-photon excitation from the ground state. To accomplish this, Stark-mixed $n = 2$ states were optically excited in electric fields. By adiabatically switching off the electric field after laser excitation, some of the mixed states evolved into pure $2\,^3S_1$ levels, whose presence was detected via the time dependence of their annihilation γ radiation. The observed $\approx 4\%$ production efficiency relative to that of Rydberg Ps states is consistent with a Monte Carlo simulation that takes into account the rate at which the electric fields were switched off.

I. INTRODUCTION

Positronium (Ps) is a hydrogenic atomic system comprising a positron bound to an electron [1]. As it is composed of a particle-antiparticle pair, Ps atoms are intrinsically metastable and can self-annihilate, converting the total rest mass of the particles into γ-ray photons. The annihilation decay rate τ^{-1} of triplet (singlet) S states is $\approx 7\,\mathrm{MHz}/n^3$ ($8\,\mathrm{GHz}/n^3$), where n refers to the principal quantum number [2,3]. While the existence of an annihilation channel does affect the intrinsic widths of some energy levels, Ps atoms are sufficiently long lived that they have a well-defined atomic structure [4]. There is much interest [5,6] in performing precision measurements of Ps energy levels [7–10] and decay rates [11–13] since they can serve as sensitive tests of bound-state QED theory [14].

New measurements of the Ps $n = 2$ fine structure [10,15,16] would benefit from an efficient source of $2\,^3S_1$ atoms. Also, some experiments employing ground-state triplet Ps atoms are limited by its short lifetime. For example, Ps scattering [17] and time-of-flight (TOF) [18] measurements could be performed with greatly improved statistics and/or resolution using longer-lived atoms. Highly excited Rydberg states [19] can be employed to accomplish this [20,21], but some experimental arrangements may not be compatible with their high sensitivity to electric fields [22] or the ease with which they can be ionized following interactions with surfaces [23]. In these cases long-lived ($\tau = 1.1\,\mu\mathrm{s}$) $2\,^3S_1$ atoms, for which radiative decay is suppressed [24], may be used instead.

Several methods of producing $2\,^3S_1$ Ps atoms have been previously demonstrated or suggested: (1) Doppler-free two-photon excitation of ground-state atoms [25–27], (2) single-photon excitation of ground-state atoms to $n = 3$ levels with subsequent radiative decay [28], and (3) collisional production following positron impact with solid [29–33] or gaseous [34,35] targets.

Recent work in which Ps atoms were excited to $n = 2$ states in electric fields [36,37] has indicated that it should be possible to produce $2\,^3S_1$ atoms by single-photon excitation. This process, which is ordinarily forbidden by electric dipole selection rules (e.g., Ref. [38]), is made possible by exciting Ps atoms in an electric field, so that Stark mixing adds some P character to $2\,^3S_1$ levels; henceforth, we refer to these mixed states as $2\,^3S_1'$ states. If the electric field in which they are produced is subsequently reduced to zero adiabatically, $2\,^3S_1'$ states can evolve into pure $2\,^3S_1$ levels.

In order to characterize $2\,^3S_1$ production we define ϵ_{2S} as the fraction of incident positrons that ultimately form $2\,^3S_1$ atoms. This parameter is sufficient for collisional techniques that generate excited-state atoms directly, but when using techniques in which ground-state atoms are converted into excited states one must take into account ϵ_{Ps}, the fraction of incident positrons that form $1\,^3S_1$ Ps atoms, and ϵ_{ex}, the fraction of available atoms that are excited. In general we may write $\epsilon_{2S} = \epsilon_{\mathrm{Ps}}\epsilon_{\mathrm{ex}}\epsilon_{\mathrm{Q}}$, where ϵ_{Q} refers to the fraction of excited atoms that subsequently form $2\,^3S_1$ states. For convenience in the following we assume $\epsilon_{\mathrm{Ps}} = 0.3$ for all cases, although it can vary considerably depending on the Ps formation target used [39].

The efficiency of two-photon excitation has an intrinsic upper limit because the 486 nm light required to drive the $1\,^3S_1 \rightarrow 2\,^3S_1$ transition is also able to photoionize $2\,^3S_1$ atoms [40]. The fraction of atoms ionized by the laser light will increase with its intensity; the photoionization rate will eventually exceed the excitation rate, reaching a steady-state equilibrium for which $\epsilon_{\mathrm{ex}} = 17.6\%$ (for both Ps and H) [41]. In this case $\epsilon_{\mathrm{Q}} = 1$, since only $2\,^3S_1$ levels are populated.

The efficiency of single-photon excitation to $3\,^3P_J$ levels, with subsequent radiative decay to the $2\,^3S_1$ level, is intrinsically limited by the branching ratio for spontaneous $3\,^3P_J \rightarrow 2\,^3S_1$ transitions. This quantity, which corresponds to ϵ_{Q}, has not been measured for Ps, but by analogy with hydrogen it is expected to be close to 12% [42]. The $1\,^3S_1 \rightarrow 3\,^3P_J$ transition has been observed [28]: $\epsilon_{\mathrm{ex}} = 15\%$ was measured, giving an estimated overall efficiency of $\epsilon_{2S} \approx 1\%$ for this method (in the absence of additional loss mechanisms).

The production of $n = 2$ Ps atoms following positron interactions with various metal or gaseous targets has been experimentally demonstrated, with a range of efficiencies observed; using atomically clean metal surfaces, efficiencies of $\approx 0.1\%$ were measured [31]. The different electron work functions associated with untreated metal surfaces appear to result in higher efficiencies of $\approx 2.5\%$ [32,33]. However, these numbers refer to the production of atoms in all $n = 2$ states, of which only 3/16 will be $2\,^3S_1$ levels. Thus, this approach yields values of $\epsilon_{2S} \approx 0.5\%$, or less. Higher $n = 2$ production efficiencies (5.7%) have been observed in positron-gas collisions [34], but again this methodology results in approximately equal production of all $n = 2$ states, and hence implies $\epsilon_{2S} \approx 1\%$. Table I lists some examples of different $2\,^3S_1$ production efficiencies.

TABLE I. Production efficiencies of 2^3S_1 Ps atoms using different techniques, as described in the text. For cases that involve exciting ground-state atoms, an experimentally realistic Ps formation fraction of $\epsilon_{Ps} = 30\%$ has been assumed. The $2^3S_1' \rightarrow 2^3S_1$ case does not include losses due to field switching times.

Method	ϵ_{2S} (%)	Comments	Ref.
e^+-metal	0.05	clean Cu(110)	[31]
e^+-metal	0.38	untreated W	[32]
e^+-metal	0.47	untreated Au	[33]
e^+-gas	1.1	H_2 gas	[34]
$1^3S_1 \rightarrow 2^3S_1$	5.3	Doppler-free	[41]
$3^3P_J \rightarrow 2^3S_1$	0.9	$\epsilon_{ex} = 0.25$	[28]
$2^3S_1' \rightarrow 2^3S_1$	1.9	$\epsilon_{ex} = 0.25$	

We report here the generation of pure 2^3S_1 atoms by adiabatic extraction of Stark-mixed states from an electric field to a field-free region. Ps atoms were optically excited in parallel electric and magnetic fields, as described elsewhere [37], except in this case the electric field is turned off immediately after the excitation has occurred. If this is done on a time scale commensurate with the lifetime of the $2^3S_1'$ states, they can evolve into pure 2^3S_1 levels. The efficiency with which this can be accomplished is limited by several factors which are discussed below; we estimate that in the present experiments we obtain $\epsilon_{2S} \approx 0.3\%$.

II. EXPERIMENTAL METHODS

The apparatus used in this work is discussed in detail elsewhere [43], as are the methods used to generate lifetime [44] and TOF spectra [45]. The main difference in the present arrangement is the placement of the detectors, and the time-varying electric fields in the target region. A two-stage Surko-type buffer gas positron trap [46] was used to produce time-bunched [47] positrons ($\Delta t \approx 4$ ns) with a repetition rate of 1 Hz. These positrons are implanted into a mesoporous silica film [48,49] that then emits Ps atoms within 10 ns [50]. We estimate that approximately 1×10^5 positrons were implanted into the target per bunch, and that 30% of these formed 1^3S_1 atoms, with energies of ≈ 100 meV. The target chamber and the position of the γ-ray detectors are shown schematically in Fig. 1.

Ps atoms emitted from the silica target were irradiated within a few millimeters of its surface by laser light. Two pulsed dye lasers were used in the experiment: $1^3S_1 \rightarrow 2^3P_J$ transitions were driven using an ultraviolet (UV) laser ($\approx 500\,\mu J$, $\Delta\nu = 85$ GHz, $\lambda = 243.0$ nm), and $2^3P_J \rightarrow n^3S/n^3D$ transitions were driven using an infrared (IR) laser (≈ 6 mJ, $\Delta\nu = 5$ GHz, $\lambda = 750$ nm). Both lasers were pumped by the same Nd:YAG laser ($\Delta t = 6$ ns FWHM). For all of the measurements we report here the UV laser light polarization was parallel to the applied electric field. Thus, only transitions for which $\Delta M_J = 0$ were driven, which is the optimal configuration for the excitation of $2^3S_1'$ states [37].

For some of the measurements reported here, Rydberg Ps atoms [19] were produced using the resonance-enhanced two-color two-photon $1^3S \rightarrow 2^3P \rightarrow n^3S/n^3D$ excitation scheme first demonstrated by Ziock and co-workers [51].
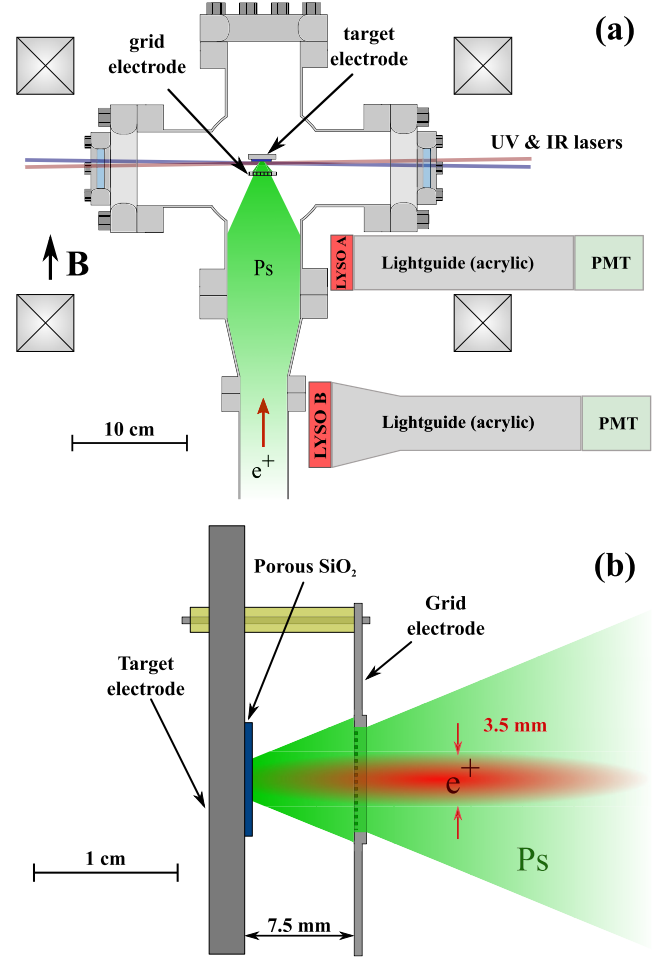
FIG. 1. Positronium formation and excitation region, showing the positions of the two LYSO detectors (a) and the target and grid electrode arrangement (b). The shaded regions represent the divergent Ps beam profile, as collimated by the grid electrode.

In general the efficiency with which $n = 2$ atoms can be transferred to Rydberg levels is high ($\geqslant 90\%$ [52]). Ps atoms were detected via their annihilation γ radiation using single-shot lifetime spectroscopy [53]. Two lutetium-yttrium oxy-orthosilicate (LYSO) scintillator based γ-ray detectors [44] were used, as indicated in Fig. 1. These were located so as to preferentially record early (LYSO A) and late (LYSO B) events.

We parametrize lifetime spectra using f, the fraction of each spectrum in a selected time region, where

$$f = \int_B^C V(t)\,dt \Big/ \int_A^C V(t)\,dt. \qquad (1)$$

The time windows used for the integration are optimized to give the best signal-to-noise ratio for a particular type of measurement [44]. Laser-induced changes in Ps decay rates are then quantified using the parameter

$$S_\gamma = (f_{bk} - f_{sig})/f_{bk}, \qquad (2)$$

where f_{bk} refers to background measurements performed without the relevant laser light present [43,44].
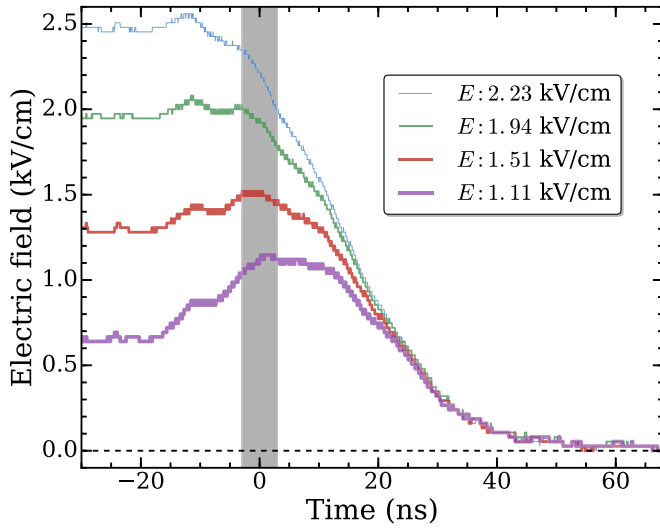
FIG. 2. Time dependence of the electric fields in the Ps excitation region, generated by switching off the target and grid electrode potentials. The shaded vertical bar indicates the time at which the laser is fired, and the temporal width of the laser pulse. The legend indicates the electric fields present at time $t = 0$ for different applied potentials.

FIG. 3. (a) Calculated energy shift, (b) fraction of $2\,^3S_1$ and $2\,^3P_J$ character, and (c) mean annihilation lifetimes of the $2\,^3S_1'$ eigenstate as a function of the electric field, with a constant parallel magnetic field of 130 G. Also shown in (a) are the Stark shifts of other $n = 2$ levels. The dashed vertical lines indicate the excitation fields used in the experiments.

The basic methodology of the present experiment is to generate $2\,^3S_1'$ atoms in an electric field, and then to reduce this field to zero before the atoms decay, allowing them to evolve into pure $2\,^3S_1$ states. These states are radiatively metastable, with a lifetime against annihilation of 1.1 μs, whereas the mean lifetime of the $2\,^3S_1'$ atoms in the fields studied is typically $\leqslant 20$ ns, determined primarily by the amount of P character they possess [37]. The rate at which the electric field in which the atoms are excited can be switched off is, therefore, a critical feature of the experiment.

The potentials applied to the target and grid electrodes [see Fig. 1(b)] were controlled by high-voltage switches that could be turned on or off with a 90–10% rise/fall time of 25 ns. The resulting electric field in the excitation region for different initial fields as a function of time is shown in Fig. 2. These data were obtained by measuring the potential applied to each electrode with a fast high-voltage probe. The probe circuit had a negligible effect on the time dependence of the applied potential, which was dominated by cable and electrode capacitances and the intrinsic properties of the high-voltage switches. The electric field was determined from the measured potentials, assuming a uniform electrode separation of 7.5 mm and neglecting any field penetration through the $\geqslant 90\%$ transmission grid.

Since the capacitance of the target electrode was slightly different from that of the grid electrode, the time dependencies of the two applied potentials were not identical, and hence a nonzero electric field was present when the potentials were switched off, as indicated in Fig. 2. To minimize the electric field variations experienced by $2\,^3S_1'$ atoms, the UV laser was fired after the switches were triggered. In this way the positron implantation energy, and thus the energy of the emitted Ps atoms [54], was the same for all electric fields studied. The effect of the varying electric fields on ground-state atoms
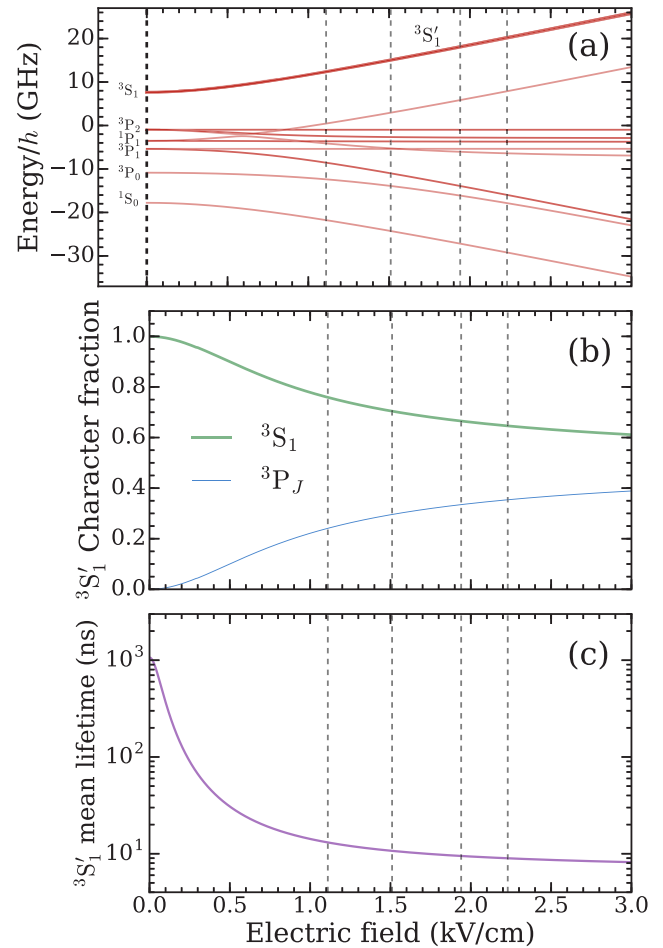
(i.e., in the time between Ps production and excitation) is negligible [37].

The time dependence of the electric fields generated in the experiments is shown in Fig. 2. Here the laser arrival time is designated as $t = 0$ and is indicated by the vertical shaded bar. The strength of the electric field present at the time of laser excitation was verified by measuring the Stark-broadened linewidth of $2\,^3P_J \rightarrow 13\,^3S/13\,^3D$ transitions for different switching times, and in static fields.

Ps atoms created in electric and magnetic fields are affected by Stark and Zeeman mixing; the energy shifts of $n = 2$ levels associated with the $\approx$kV cm^{-1} electric fields are much larger than those arising from the 130 G magnetic field [37], despite the large Ps speeds [55–57]. Calculated Stark energies of the $n = 2$ eigenstates are shown in Fig. 3(a), with the $2\,^3S_1'$ level indicated by the bold line. In order to produce pure $2\,^3S_1$ atoms it is necessary to perform the excitation in an electric field that provides sufficient coupling to the $2\,^3S_1'$ state (via its P component), and then to lower the field on a time scale commensurate with the lifetime of the $2\,^3S_1'$ states. The

fraction of P character, and hence the $2\,^3S_1'$ lifetime, depends on the electric field strength, as shown in Figs. 3(b) and 3(c). The energies and lifetimes in the presence of electric and magnetic fields were determined from the eigenvalues and eigenvectors of the complete $n = 2$ Hamiltonian matrix using the procedures described in Ref. [37].

III. RESULTS AND DISCUSSION

The primary goal of the experiments we describe here is to demonstrate that pure $2\,^3S_1$ Ps atoms can be produced from $2\,^3S_1'$ atoms under typical experimental conditions, and to evaluate the efficacy of the process. In general the excitation of $n = 2$ states leads to a small ($\lesssim 10$ ns) increase in the mean lifetime [37] that is not usually resolvable using single-shot lifetime methods [44]. However, if additional processes occur, such as magnetic quenching, photoionization, or Rydberg production [43], there will be significant changes to the mean decay rates which can be observed in lifetime spectra. Since the $2\,^3S_1$ level is radiatively metastable [24], its lifetime (1.1 μs) is determined primarily by self-annihilation. Thus, the presence of these atoms can also be observed via single-shot lifetime spectroscopy.

By exciting Ps atoms with two lasers (UV + IR) it is possible to generate highly excited Rydberg states [51,52]. In our current apparatus we have demonstrated the production of states with principal quantum numbers ranging from $n = 8$ to the ionization limit [58]. The annihilation rate of Ps Stark states with $n = 8$ is negligible, but their fluorescence lifetime is $\approx 1\,\mu$s [45]. This is sufficiently close to the 1.1 μs annihilation lifetime of $2\,^3S_1$ atoms that measurements employing $n = 8$ Rydberg atoms can provide a signal that has characteristics similar to those expected for the $2\,^3S_1$ atoms, but with a much higher production efficiency.

Lifetime spectra recorded with the UV and IR lasers tuned to excite $n = 8$ states are shown in Fig. 4(a). The curve in Fig. 4(b) is the difference between lifetime spectra recorded with and without IR laser light present. These data indicate laser-induced changes in the annihilation γ-ray flux, such that a positive signal represents excess annihilation events, while negative signals represent fewer annihilation events, with respect to the decay rate of ground state atoms. The initial decrease in the signal in Fig. 4(b) comes from the nonannihilation of ground-state atoms that have been excited to long-lived Rydberg states. The peak at 100 ns is due to Rydberg atoms that annihilate after colliding with the grid electrode, and the large signal peaking near 500 ns is caused by $n = 8$ atoms which either collide with the chamber wall or self-annihilate following radiative decay to their ground state.

The time dependence of the annihilation radiation signal shown in Fig. 4(b) is consistent with the physical geometry of the electrode structure and target chamber walls and the mean speed of Ps atoms emitted from the silica target ($\approx 1 \times 10^7$ cm s^{-1}). The underlying Ps velocity and angular distributions will be very similar for both $n = 2$ and $n = 8$ atoms because Doppler velocity selection by the excitation lasers is dominated by the UV laser bandwidth. Therefore, the data in Fig. 4 are expected to give a good indication of the qualitative form of a $2\,^3S_1$ signal, as long as additional annihilation channels are not present.
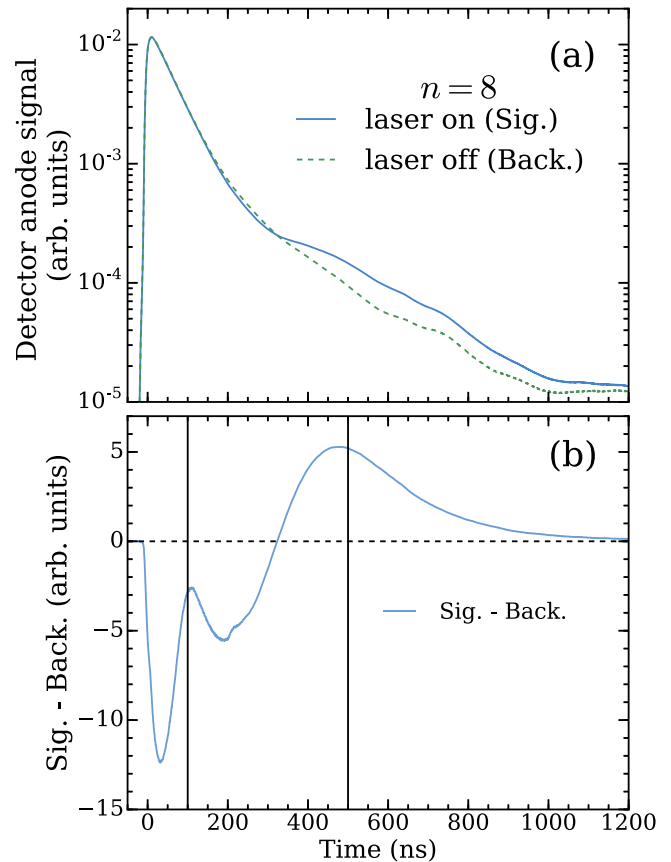

FIG. 4. (a) Lifetime spectra measured using LYSO A with and without IR laser light present. For these measurements the lasers were tuned to drive transitions to the $n = 8$ state. The difference between the laser on and off curves of (a) are shown in (b). The vertical lines at 100 and 500 ns indicate the approximate times of Ps annihilations occurring following collisions with the grid electrode and the chamber walls, respectively. The data comprise 29 000 pairs of shots and were acquired in 17 h in a nominally zero electric field.

We do in fact observe a similar annihilation radiation spectrum when measurements are performed in a configuration expected to result in the production of $2\,^3S_1$ atoms. The data in Fig. 5(a) were recorded using only a UV excitation laser, with an electric field of 2.23 kV cm^{-1}. When the electric field is switched off after excitation an excess annihilation signal peaking at ≈ 500 ns is observed, which bears a strong similarity to the data of Fig. 4(b). Using a static field that is always present, no excess signal is observed. The same measurement was performed in an electric field of 1.11 kV cm^{-1} [Fig. 5(b)] and an excess signal was again observed. In this case, however, because of the low excitation field there is also a magnetic quenching signal present. This signal is visible as an increase in annihilation events at early times [37] and is relatively strong, making the $2\,^3S_1$ signal appear less prominent. However, as can be seen in the inset to Fig. 5(b), the magnitude of the delayed signal is comparable to that observed for higher fields. Similar measurements were also performed for fields of 1.51 and 1.94 kV cm^{-1} (see Fig. 2).

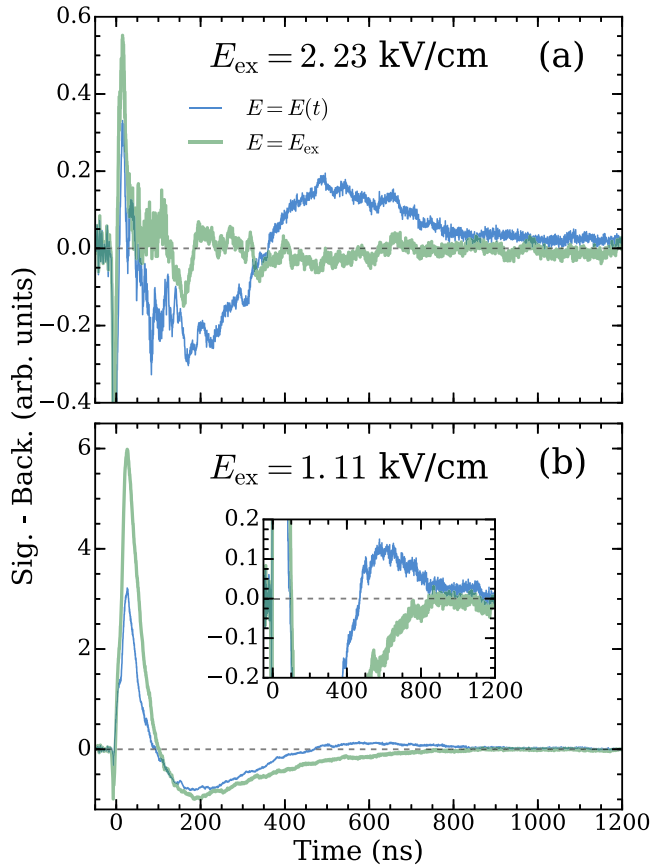The presence of long-lived Ps atoms can also be detected via single-event counting using LYSO B (see Fig. 1). This

FIG. 5. Difference curves recorded using LYSO A for excitation fields E_{ex} of (a) $2.23 \, \text{kV cm}^{-1}$ and (b) $1.11 \, \text{kV cm}^{-1}$. Data are shown for fields that are switched off $[E = E(t)]$ and that are held at the excitation field $[E = E_{ex}]$. The inset in (b) shows the delayed signal attributed to $2^3 S_1$ atoms on an expanded scale. Each curve is the average of approximately 13 000 shots and was acquired in 3.7 h.
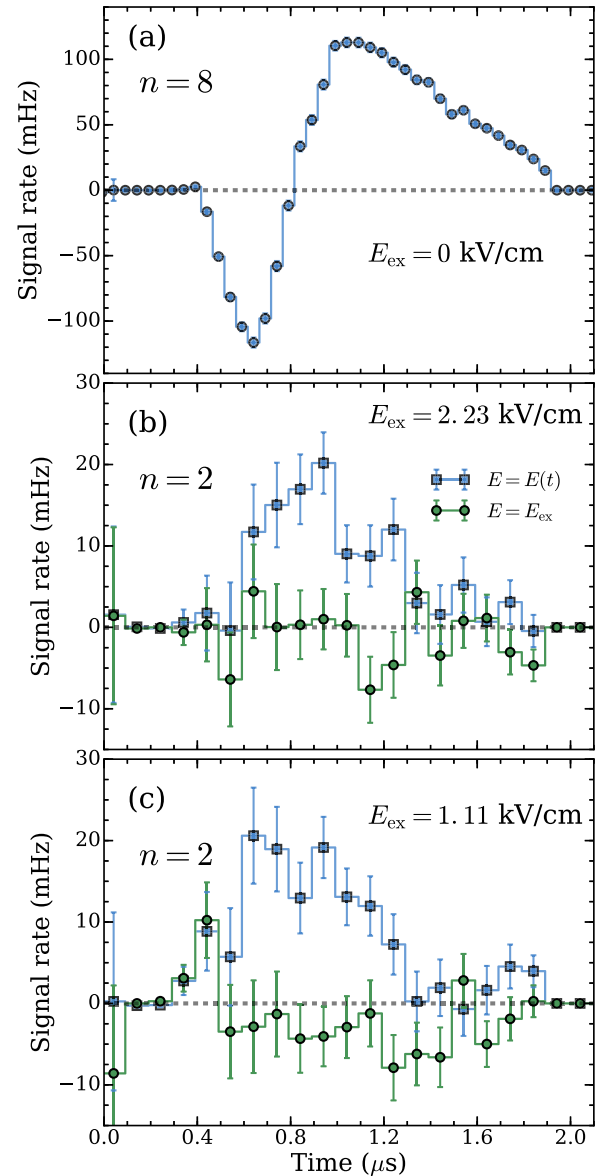

FIG. 6. TOF spectra recorded by LYSO B with lasers tuned to excite (a) $n = 8$ Rydberg states or (b), (c) $n = 2$ states. The spectra are background subtracted as described in the text. Data were recorded in different electric fields, as indicated in each panel, and for the $n = 2$ data for cases with the fields switched off $[E = E(t)$, squares] or for static fields $[E = E_{ex}$, circles].

detector is farther away from the Ps target and is therefore more sensitive to delayed annihilation events. A single-event counting procedure was used to produce TOF spectra, as described in Ref. [45]. TOF data are shown in Fig. 6; these were recorded at the same time as the data shown in Figs. 4 and 5. The TOF spectra have been background subtracted, where the background corresponds to the case where no laser light is present.

As in the single-shot lifetime data, the production of $n = 8$ atoms can provide a proxy signal that will have similar qualitative properties to that expected for $2^3 S_1$ atoms. Figure 6(a) shows TOF data recorded with the UV and IR lasers tuned to excite $n = 8$ atoms. For these data the background subtraction procedure results in a negative peak at early times in the distribution because the transfer of ground-state atoms to Rydberg levels is so efficient that it significantly depletes the background population. By extrapolating over this negative region, however, one can infer that the distribution exhibits a peak in the region of $1 \, \mu\text{s}$.

TOF spectra recorded under conditions where $2^3 S_1$ production is expected are shown in Figs. 6(b) and 6(c) [cf. Figs. 5(a) and 5(b)]. As observed in the lifetime spectra, a delayed signal is present when the electric fields are switched

off, but not when the fields are maintained after laser excitation has occurred. Thus, these data confirm the observation that $2^3 S_1$ atoms have been produced. As with the lifetime spectra, TOF spectra (not shown) were also recorded in electric fields of 1.51 and $1.94 \, \text{kV cm}^{-1}$, yielding similar results.

The production efficiency of $2^3 S_1$ atoms can be quantified using the parameter S_γ [see Eq. (2)]. The values of S_γ obtained using LYSO A for different electric fields, and with the fields switched, are shown in Fig. 7. The definition of S_γ is such that early annihilation events (i.e., ionization or magnetic quenching) yield a positive value, whereas the creation of long-lived atoms yields a negative value. The absolute value of S_γ is arbitrary and depends on several factors, including the time windows chosen for the integration [44]. However,
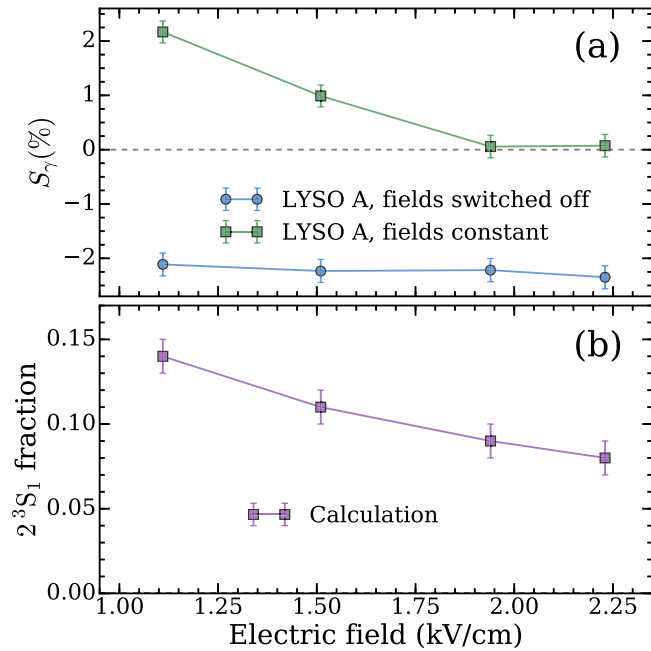
FIG. 7. (a) S_γ values obtained from lifetime spectra of Fig. 5 with and without switching off the electric field and (b) the calculated fraction of $2\,^3S_1'$ atoms that remain as $2\,^3S_1$ states, obtained using the measured time-dependent electric fields.
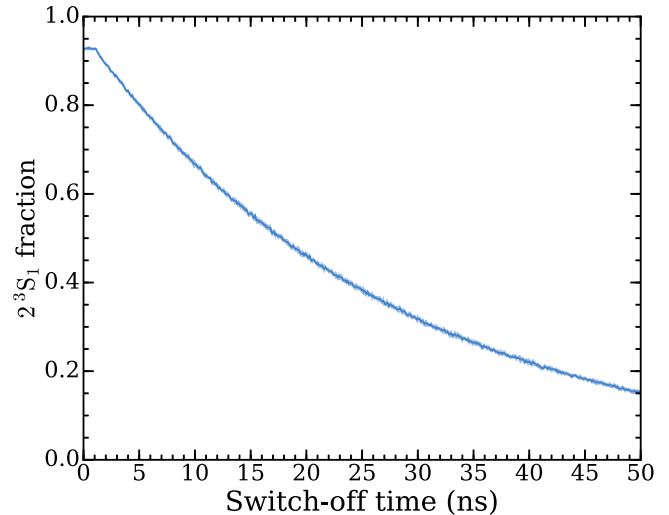

FIG. 8. Calculated fraction of $2\,^3S_1'$ states surviving as $2\,^3S_1$ states as a function of the time taken to switch the field off (see text for details). The atoms were initially prepared in an electric field of $1.1\,\mathrm{kV\,cm^{-1}}$.

for a given detector configuration, and using fixed integration regions, one can compare different S_γ measurements to infer a relative yield of long-lived states. The positive value of S_γ shown in Fig. 7(a) for low static electric fields arises through magnetic quenching. In this process Zeeman mixing couples singlet and triplet states, leading to an increased annihilation rate following excitation to $n = 2$. This effect can be enhanced by Stark mixing but becomes negligible at higher electric fields for the experimental conditions used in this work [37].

The data shown in Fig. 4 correspond to $S_\gamma = -60\%$, using time windows of $A = -5$, $B = 400$, and $C = 1200$ ns [see Eqs. (1) and (2)]. The $2\,^3S_1$ production as measured via S_γ does not appear to depend strongly on the electric field, as shown in Fig. 7(a). The average value obtained $S_\gamma = -2.2 \pm 0.4\%$ indicates that the production efficiency of $2\,^3S_1$ atoms compared to Rydberg atoms was about 4%. If all of the accessible $n = 2$ states are produced with equal probability then, considering the allowed transitions and the laser polarization used [37], the fraction of those in $2\,^3S_1'$ states would be 25% (i.e., $\epsilon_Q = 0.25$). If we assume that almost all $n = 2$ states are transferred to Rydberg levels [52] then we would expect to measure $S_\gamma \approx -15\%$. The observed $S_\gamma = -2.2\%$ therefore suggests that an additional loss mechanism may be present.

Further information on the $2\,^3S_1$ production efficiency was obtained by comparison of the experimental data with the results of Monte Carlo simulations of the evolution of the excited atoms in the time-dependent fields in Fig. 2. In the excitation fields used in the experiments the ^3P character of the $2\,^3S_1'$ state ranges from to 0.24 to 0.35. For the typical laser intensity of $5 \times 10^5\,\mathrm{W\,cm^{-2}}$ used in the experiments, the Rabi frequencies of the $1\,^3S_1 \to 2\,^3S_1'$ transitions with

these fractions of ^3P character range from to 9 to 13 GHz. Consequently, within the 6-ns duration of the excitation laser pulse, the transition to the $2\,^3S_1'$ state is saturated for each of the excitation fields in the experiments. This was accounted for in the Monte Carlo simulations by considering a fixed number (1×10^4) of initially excited atoms in the $2\,^3S_1'$ state. The simulation then proceeded from this excitation time, $t = 0$, for 80 ns. At each 1-ns time interval the instantaneous decay rate of the $2\,^3S_1'$ state was evaluated in the corresponding electric field (see Fig. 3). For each $2\,^3S_1'$ atom the decay probability was then compared to a randomly generated number between zero and 1 to determine if it remained excited or decayed to the $1\,^3S_1$ level. After the evolution time of 80 ns the time-dependent electric fields displayed in Fig. 2 were all sufficiently small that the $2\,^3S_1'$ decay rate was approximately equal to that of the pure $2\,^3S_1$ level.

The simulation was used to determine the fraction of the initially prepared atoms that remained in the $2\,^3S_1$ level after 80 ns. For the excitation fields of 1.11, 1.51, 1.94, and $2.23\,\mathrm{kV\,cm^{-1}}$ used in the experiments, the calculated $2\,^3S_1$ fractions were 0.14, 0.11, 0.09, and 0.08 ± 0.01, respectively, as shown in Fig. 7(b). No significant difference in the $2\,^3S_1$ yields were observed for these fields, while the simulation suggests that the extraction efficiency should be higher at lower excitation fields. This discrepancy is not presently understood, but may be related to optical pumping effects (not included in the simulation) that increase the fraction of atoms that can be excited to $2\,^3S_1'$ states as the field is increased.

The simulation was also used to investigate the overall dependence of the surviving fraction of $2\,^3S_1$ atoms on the rate at which the excitation field is switched off. The surviving fraction was calculated for an excitation field of $1.11\,\mathrm{kV\,cm^{-1}}$, and different field switch-off times, assuming a linear time dependence. The results, shown in Fig. 8, imply that the experimentally attained $2\,^3S_1$ survival efficiency of ~0.15 could be increased to more than 0.9 if the time in which the electric field is switched from $1.11\,\mathrm{kV\,cm^{-1}}$ to

zero was reduced to ≈ 2 ns. This is in principle possible if the electrodes are redesigned with lower capacitances and by employing a faster high-voltage switch (e.g., Ref. [59]). From Landau-Zener theory [60,61], the time evolution of the $2\,^3S_1'$ state to the pure $2\,^3S_1$ level in zero field remains adiabatic; i.e., the probability of diabatic evolution is less than 0.01, for all switch-off times exceeding 0.05 ns ($dE/dt < 22\,\mathrm{kV\,cm^{-1}\,ns^{-1}}$).

IV. CONCLUSIONS

We have verified that $2\,^3S_1$ Ps atoms can be produced using single-photon excitation from the ground state in an electric field. We observe a production efficiency of 3.8%, relative to the production of Rydberg levels. This is much less than the $\approx 25\%$ we would expect assuming complete transfer of all $n = 2$ states to Rydberg states [52], and without losses due to the field switching times. A Monte Carlo simulation was performed to evaluate the extent of such losses, and it was found that in our experimental conditions the expected 25% would be reduced to around 3.5%. Our data are therefore consistent with the results of the simulation, although the observed field-independent yield is not explained.

We estimate that in our experiments $\epsilon_{\mathrm{ex}} \approx 0.25$ and $\epsilon_{\mathrm{Ps}} \approx 0.3$. For $\epsilon_Q \approx 0.25$ (i.e., the ideal case without switching losses) the maximum yield per positron is then $\epsilon_{2S} \approx 1.9\%$. As indicated in Table I, this efficiency is around twice as large as the (as yet undemonstrated) excitation scheme employing transitions to $n = 3$ [28], and is two to four times higher than the yield expected from collisional methods, largely because they are not state selective.

Using gaseous targets will generally result in the generation of $n = 2$ Ps atoms with energies of several eV or more [34]. Excited-state Ps emitted from metals is primarily generated from epithermal or backscattered positrons and, therefore, also has energies in the 1–10 eV range [62]. These fast atoms are not desirable for all applications; for example, the precision attainable in Ps fine-structure measurements could be limited by associated Doppler shifts and/or transit-time effects using such energetic atoms. However, these methods do have the advantage that they require neither lasers nor a pulsed positron beam to produce excited states of Ps.

Even without losses arising from long switching times, the estimated production efficiency using the method we have discussed here is lower than could be obtained by direct two-photon excitation (5.3%). This method is in principle the most efficient, although it does require high-power, narrow-band lasers. To achieve this maximal efficiency the bandwidth of the laser light used must be narrower than the width of the $1\,^3S_1 \rightarrow 2\,^3S_1$ transition (i.e., 1.3 MHz), otherwise more laser power will be available to photoionize than to drive the transition.

Increasing the Ps production efficiency would increase the absolute $2\,^3S_1$ yield. In this work we have assumed $\epsilon_{\mathrm{Ps}} = 30\%$ to facilitate comparisons of different methods and our data. The actual Ps production efficiency in a given experiment can vary considerably [39]. By using hot metal targets, for example, it is possible to obtain $\epsilon_{\mathrm{Ps}} \approx 75\%$ [18], which corresponds to 100% Ps formation, since 25% of all Ps formed will be in the singlet state. Thus one could in principle increase the $2\,^3S_1$ yield for ground-state Ps-mediated production listed in Table I by a factor of 2.5.

The ability to produce $2\,^3S_1$ atoms in a simple and efficient way would be useful for several experimental programs. Our primary motivation is to conduct new precision measurements of the Ps fine structure [10,15,16]. By combining the techniques described here with Doppler correction methods [63] it may be possible to measure various microwave transitions in the $n = 2$ manifold to ≈ 100 kHz, increasing the precision of previous work by an order of magnitude. Furthermore, access to long-lived states that are insensitive to external fields could make it possible to perform Ps interferometry measurements [64] using physical gratings [65], which may not be compatible with Rydberg atoms [66].

ACKNOWLEDGMENTS

[1] J. A. Wheeler, Polyelectrons, Ann. N.Y. Acad. Sci. **48**, 219 (1946).

[2] P. A. M. Dirac, On the annihilation of electrons and protons, Math. Proc. Cambridge Philos. Soc. **26**, 361 (1930).

[3] A. Ore and J. L. Powell, Three-photon annihilation of an electron-positron pair, Phys. Rev. **75**, 1696 (1949).

[4] H. A. Bethe and E. E. Salpeter, *Quantum Mechanics of One- and Two-Electron Atoms* (Springer, Berlin, 1957).

[5] S. Berko and H. N. Pendleton, Positronium, Annu. Rev. Nucl. Part. Sci. **30**, 543 (1980).

[6] A. Rich, Recent experimental advances in positronium research, Rev. Mod. Phys. **53**, 127 (1981).

[7] M. S. Fee, A. P. Mills, Jr., S. Chu, E. D. Shaw, K. Danzmann, R. J. Chichester, and D. M. Zuckerman, Measurement of the Positronium $1\,^3S_1 - 2\,^3S_1$ Interval by Continuous-Wave Two-Photon Excitation, Phys. Rev. Lett. **70**, 1397 (1993).

[8] M. W. Ritter, P. O. Egan, V. W. Hughes, and K. A. Woodle, Precision determination of the hyperfine-structure interval in the ground state of positronium. V, Phys. Rev. A **30**, 1331 (1984).

[9] A. Ishida, T. Namba, S. Asai, T. Kobayashi, H. Saito, M. Yoshida, K. Tanaka, and A. Yamamoto, New precision measurement of hyperfine splitting of positronium, Phys. Lett. B **734**, 338 (2014).

[10] A. P. Mills, Jr., S. Berko, and K. F. Canter, Fine-Structure Measurement in the First Excited State of Positronium, Phys. Rev. Lett. **34**, 1541 (1975).

[11] R. S. Vallery, P. W. Zitzewitz, and D. W. Gidley, Resolution of the Orthopositronium-Lifetime Puzzle, Phys. Rev. Lett. **90**, 203402 (2003).

[12] O. Jinnouchi, S. Asai, and T. Kobayashi, Precision measurement of orthopositronium decay rate using SiO$_2$ powder, Phys. Lett. B **572**, 117 (2003).

[13] Y. Kataoka, S. Asai, and T. Kobayashi, First test of correction of the orthopositronium decay rate, Phys. Lett. B **671**, 219 (2009).

[14] S. G. Karshenboim, Precision study of positronium: Testing bound state QED theory, Int. J. Mod. Phys. A **19**, 3879 (2004).

[15] S. Hatamian, R. S. Conti, and A. Rich, Measurements of the $2\,^3S_1 - 2^3P_J$ ($J = 0,1,2$) Fine-Structure Splittings in Positronium, Phys. Rev. Lett. **58**, 1833 (1987).

[16] D. Hagena, R. Ley, D. Weil, G. Werth, W. Arnold, and H. Schneider, Precise Measurement of $n = 2$ Positronium Fine-Structure Intervals, Phys. Rev. Lett. **71**, 2887 (1993).

[17] S. J. Brawley, S. E. Fayer, M. Shipman, and G. Laricchia, Positronium Production and Scattering Below Its Breakup Threshold, Phys. Rev. Lett. **115**, 223201 (2015).

[18] A. P. Mills, Jr. and L. Pfeiffer, Desorption of Surface Positrons: A Source of Free Positronium at Thermal Velocities, Phys. Rev. Lett. **43**, 1961 (1979).

[19] T. F. Gallagher, *Rydberg Atoms* (Cambridge University Press, Cambridge, UK, 1994).

[20] A. C. L. Jones, H. J. Goldman, Q. Zhai, P. Feng, H. W. K. Tom, and A. P. Mills, Monoenergetic Positronium Emission from Metal-Organic Framework Crystals, Phys. Rev. Lett. **114**, 153201 (2015).

[21] A. C. L. Jones, H. J. Rutbeck-Goldman, T. H. Hisakado, A. M. Piñeiro, H. W. K. Tom, A. P. Mills, B. Barbiellini, and J. Kuriplach, Angle-Resolved Spectroscopy of Positronium Emission from a Cu(110) Surface, Phys. Rev. Lett. **117**, 216402 (2016).

[22] A. Osterwalder and F. Merkt, Using High Rydberg States as Electric Field Sensors, Phys. Rev. Lett. **82**, 1831 (1999).

[23] Y. Pu, D. D. Neufeld, and F. B. Dunning, Ionization of Rydberg atoms at metallic surfaces: Influence of stray fields, Phys. Rev. A **81**, 042904 (2010).

[24] G. Breit and E. Teller, Metastability of hydrogen and helium Levels, Astrophys. J. **91**, 215 (1940).

[25] S. Chu and A. P. Mills, Jr., Excitation of the Positronium $1^3S_1 \to 2^3S_1$ Two-Photon Transition, Phys. Rev. Lett. **48**, 1333 (1982).

[26] M. S. Fee, S. Chu, A. P. Mills, R. J. Chichester, D. M. Zuckerman, E. D. Shaw, and K. Danzmann, Measurement of the positronium $1\,^3S_1 - 2\,^3S_1$ interval by continuous-wave two-photon excitation, Phys. Rev. A **48**, 192 (1993).

[27] D. Cooke, P. Crivelli, J. Alnis, A. Antognini, B. Brown, S. Friedreich, A. Gabard, T. W. Haensch, K. Kirch, A. Rubbia, and V. Vrankovic, Observation of positronium annihilation in the 2S state: Towards a new measurement of the 1S–2S transition frequency, Hyperfine Int. **233**, 67 (2015).

[28] S. Aghion, C. Amsler, A. Ariga, T. Ariga, G. Bonomi, P. Bräunig, J. Bremer, R. S. Brusa, L. Cabaret, M. Caccia, R. Caravita, F. Castelli, G. Cerchiari, K. Chlouba, S. Cialdi, D. Comparat, G. Consolati, A. Demetrio, L. Di Noto, M. Doser, A. Dudarev, A. Ereditato, C. Evans, R. Ferragut, J. Fesel, A. Fontana, O. K. Forslund, S. Gerber, M. Giammarchi, A. Gligorova, S. Gninenko, F. Guatieri, S. Haider, H. Holmestad, T. Huse, I. L. Jernelv, E. Jordan, A. Kellerbauer, M. Kimura, T. Koettig, D. Krasnicky, V. Lagomarsino, P. Lansonneur, P. Lebrun, S. Lehner, J. Liberadzka, C. Malbrunot, S. Mariazzi, L. Marx, V. Matveev, Z. Mazzotta, G. Nebbia, P. Nedelec, M. Oberthaler, N. Pacifico, D. Pagano, L. Penasa, V. Petracek, C. Pistillo, F. Prelz,

M. Prevedelli, L. Ravelli, L. Resch, B. Rienäcker, O. M. Røhne, A. Rotondi, M. Sacerdoti, H. Sandaker, R. Santoro, P. Scampoli, L. Smestad, F. Sorrentino, M. Spacek, J. Storey, I. M. Strojek, G. Testera, I. Tietje, S. Vamosi, E. Widmann, P. Yzombard, J. Zmeskal, and N. Zurlo (AEgIS Collaboration), Laser excitation of the $n = 3$ level of positronium for antihydrogen production, Phys. Rev. A **94**, 012507 (2016).

[29] K. F. Canter, A. P. Mills, Jr., and S. Berko, Observations of Positronium Lyman-α Radiation, Phys. Rev. Lett. **34**, 177 (1975).

[30] R. Ley, K. D. Niebling, R. Schwarz, and G. Werth, Evidence from $n = 2$ fine structure transitions for the production of fast excited state positronium, J. Phys. B **23**, 1915 (1990).

[31] D. C. Schoepf, S. Berko, K. F. Canter, and P. Sferlazzo, Observation of Ps ($n = 2$) from well-characterized metal surfaces in ultrahigh vacuum, Phys. Rev. A **45**, 1407 (1992).

[32] T. D. Steiger and R. S. Conti, Formation of $n = 2$ positronium from untreated metal surfaces, Phys. Rev. A **45**, 2744 (1992).

[33] D. J. Day, M. Charlton, and G. Laricchia, On the formation of excited state positronium in vacuum by positron impact on untreated surfaces, J. Phys. B **34**, 3617 (2001).

[34] G. Laricchia, M. Charlton, G. Clark, and T. C. Griffith, Excited state positronium formation in low density gases, Phys. Lett. A **109**, 97 (1985).

[35] D. J. Murtagh, D. A. Cooke, and G. Laricchia, Excited-State Positronium Formation from Helium, Argon, and Xenon, Phys. Rev. Lett. **102**, 133202 (2009).

[36] A. M. Alonso, B. S. Cooper, A. Deller, S. D. Hogan, and D. B. Cassidy, Controlling Positronium Annihilation with Electric Fields, Phys. Rev. Lett. **115**, 183401 (2015).

[37] A. M. Alonso, B. S. Cooper, A. Deller, S. D. Hogan, and D. B. Cassidy, Positronium decay from $n = 2$ states in electric and magnetic fields, Phys. Rev. A **93**, 012506 (2016).

[38] W. Demtröder, *Laser Spectroscopy*, 3rd ed. (Springer, New York, 2003).

[39] P. J. Schultz and K. G. Lynn, Interaction of positron beams with surfaces, thin films, and interfaces, Rev. Mod. Phys. **60**, 701 (1988).

[40] S. Chu, A. P. Mills, Jr., and J. L. Hall, Measurement of the Positronium $1\,^3S_1 - 2\,^3S_1$ Interval by Doppler-Free Two-Photon Spectroscopy, Phys. Rev. Lett. **52**, 1689 (1984).

[41] M. Haas, U. D. Jentschura, C. H. Keitel, N. Kolachevsky, M. Herrmann, P. Fendel, M. Fischer, Th. Udem, R. Holzwarth, T. W. Hänsch, M. O. Scully, and G. S. Agarwal, Two-photon excitation dynamics in bound two-body Coulomb systems including ac Stark shift and ionization, Phys. Rev. A **73**, 052501 (2006).

[42] K. C. Harvey, Slow metastable atomic hydrogen beam by optical pumping, J. Appl. Phys. **53**, 3383 (1982).

[43] B. S. Cooper, A. M. Alonso, A. Deller, T. E. Wall, and D. B. Cassidy, A trap-based pulsed positron beam optimised for positronium laser spectroscopy, Rev. Sci. Instrum. **86**, 103101 (2015).

[44] A. M. Alonso, B. S. Cooper, A. Deller, and D. B. Cassidy, Single-shot positron annihilation lifetime spectroscopy with LYSO scintillators, Nucl. Instrum. Methods Phys. Res. Sect. A **828**, 163 (2016).

[45] A. Deller, A. M. Alonso, B. S. Cooper, S. D. Hogan, and D. B. Cassidy, Measurement of Rydberg positronium fluorescence lifetimes, Phys. Rev. A **93**, 062513 (2016).

[46] J. R. Danielson, D. H. E. Dubin, R. G. Greaves, and C. M. Surko, Plasma and trap-based techniques for science with positrons, Rev. Mod. Phys. **87**, 247 (2015).

[47] A. P. Mills, Jr., Time bunching of slow positrons for annihilation lifetime and pulsed laser photon absorption experiments, Appl. Phys. **22**, 273 (1980).

[48] L. Liszkay, M. F. Barthe, C. Corbel, P. Crivelli, P. Desgardin, M. Etienne, T. Ohdaira, P. Perez, R. Suzuki, V. Valtchev, and A. Walcarius, Orthopositronium annihilation and emission in mesostructured thin silica and silicalite-1 films, Appl. Surf. Sci. **255**, 187 (2008).

[49] L. Liszkay, F. Guillemot, C. Corbel, J.-P. Boilot, T. Gacoin, E. Barthel, P. Prez, M.-F. Barthe, P. Desgardin, P. Crivelli, U. Gendotti, and A. Rubbia, Positron annihilation in latex-templated macroporous silica films: Pore size and ortho-positronium escape, New J. Phys. **14**, 065009 (2012).

[50] A. Deller, B. S. Cooper, T. E. Wall, and D. B. Cassidy, Positronium emission from mesoporous silica studied by laser-enhanced time-of-flight spectroscopy, New J. Phys. **17**, 043059 (2015).

[51] K. P. Ziock, R. H. Howell, F. Magnotta, R. A. Failor, and K. M. Jones, First Observation of Resonant Excitation of High-n States in Positronium, Phys. Rev. Lett. **64**, 2366 (1990).

[52] D. B. Cassidy, T. H. Hisakado, H. W. K. Tom, and A. P. Mills, Jr., Efficient Production of Rydberg Positronium, Phys. Rev. Lett. **108**, 043401 (2012).

[53] D. B. Cassidy, S. H. M. Deng, H. K. M. Tanaka, and A. P. Mills, Jr., Single shot positron annihilation lifetime spectroscopy, Appl. Phys. Lett. **88**, 194105 (2006).

[54] D. B. Cassidy, P. Crivelli, T. H. Hisakado, L. Liszkay, V. E. Meligne, P. Perez, H. W. K. Tom, and A. P. Mills, Jr., Positronium cooling in porous silica measured via Doppler spectroscopy, Phys. Rev. A **81**, 012715 (2010).

[55] S. M. Curry, Combined Zeeman and motional Stark effects in the first excited state of positronium, Phys. Rev. A **7**, 447 (1973).

[56] C. D. Dermer and J. C. Weisheit, Perturbative analysis of simultaneous Stark and Zeeman effects on $n = 1 \rightarrow n = 2$ radiative transitions in positronium, Phys. Rev. A **40**, 5526 (1989).

[57] A. C. L. Jones, T. H. Hisakado, H. J. Goldman, H. W. K. Tom, and A. P. Mills, Jr., Polarization dependence of $n = 2$ positronium transition rates to Stark-split $n = 30$ levels via crossed-beam spectroscopy, J. Phys. B **49**, 064006 (2016).

[58] T. E. Wall, A. M. Alonso, B. S. Cooper, A. Deller, S. D. Hogan, and D. B. Cassidy, Selective Production of Rydberg-Stark States of Positronium, Phys. Rev. Lett. **114**, 173001 (2015).

[59] D. B. Cassidy, S. H. M. Deng, R. G. Greaves, and A. P. Mills, Jr., Accumulator for the production of intense positron pulses, Rev. Sci. Instrum. **77**, 073106 (2006).

[60] L. D. Landau, Zur Theorie der Energieübertragung ii, Phys. Z. Sowjetunion **2**, 46 (1932).

[61] C. Zener, Non-adiabatic crossing of energy levels, Proc. R. Soc. London A **137**, 696 (1932).

[62] R. Ley, K. D. Niebling, G. Werth, C. Hahn, H. Schneider, and I. Tobehn, Energy dependence of excited positronium formation at a molybdenum surface, J. Phys. B **23**, 3437 (1990).

[63] A. C. L. Jones, T. H. Hisakado, H. J. Goldman, H. W. K. Tom, A. P. Mills, Jr., and D. B. Cassidy, Doppler-corrected Balmer spectroscopy of Rydberg positronium, Phys. Rev. A **90**, 012503 (2014).

[64] M. K. Oberthaler, Anti-matter wave interferometry with positronium, Nucl. Instrum. Methods Phys. Res. Sect. B **192**, 129 (2002).

[65] S. Sala, F. Castelli, M. Giammarchi, S. Siccardi, and S. Olivares, Matter-wave interferometry: Towards antimatter interferometers, J. Phys. B **48**, 195002 (2015).

[66] C. Fabre, M. Gross, J. M. Raimond, and S. Haroche, Measuring atomic dimensions by transmission of Rydberg atoms through micrometre size slits, J. Phys. B **16**, L671 (1983).